ENGINEERING TRANSACTIONS • *Engng. Trans.* • **41**, 1, 31–50, 1993
Polish Academy of Sciences • Institute of Fundamental Technological Research

HIGH-SPEED BOUNDARY-LAYER STABILITY AND TRANSITION

V. I. LYSENKO (NOVOSIBIRSK)

In this paper peculiarities of the laminar hypersonic (Mach numbers 4-16) boundary layer stability and its transition to the turbulent one are studied experimentally and numerically at different facilities. The influence of various factors on the boudary-layer stability and the transition is considered.

NOTATION

A_f disturbance amplitude of the frequency f,
b bluntness,
e hot-wire voltage fluctuations,
F dimensionless frequency parameter,
f disturbance frequency,
h obstacle height,
M Mach number,
n coefficient of disturbances amplification,
P_0' gauge-measured full pressure,
$R = (\mathrm{Re})^{0.5}$ Reynolds number,
R_t transition Reynolds number,
Re_1 unit Reynolds number,
T_0 stagnation temperature,
T_w temperature factor (wall-to-adiabatic wall temperature ratio),
u velocity,
x, y longitudinal and normal coordinates,
α ionization rate,
α_i disturbance amplification rates,
β velocity gradient,
γ ratio of specific heats,
δ thickness of the boundary layer,
η dimensionless normal coordinate,
ν viscosity,
χ angle of disturbance propagation.

1. Introduction

For a number of applications it is important to know the location of the hypersonic boundary-layer transition from laminar to turbulent. At present it is generally recognized that the onset of turbulence is directly connected with the loss of stability of the initial laminar flow. The boundary-layer stability and the transition are considerably affected by various factors, and such an influence is considered in the present work.

This paper is the review of author's recent papers in Russian. The investigations were carried out at the Institute of Theoretical and Applied Mechanics of the Siberian Branch of the Russian Academy of Sciences. The hotshot, nitrogen, wind tunnels and shock tube were used. The influence of Mach number, temperature factor, stagnation temperature, pressure gradient, ratio of specific heats, entropy layer, dissociation, ionization and magnetic field on the high-speed boundary-layer stability and the transition were studied. The problem of turbulization of a stable hypersonic boundary layer by means of an obstacle was considered as well.

2. The influence of the Mach number, temperature factor, stagnation temperature and pressure gradient on the stability and the transition

The calculations of the boundary layer stability and its transition were performed using the e^{n}[(1)] method at different values of the Mach number M and the temperature factor T_w (the wall-to-adiabatic wall temperature ratio). For details of the computations see Lysenko [1]. The calculations were carried out for disturbances of the first (analogous to the well-known Tollmien – Schlichting waves of an incompressible fluid) and the second (a variety of acoustic resonances in a shear flow) unstable modes. For the numerical integration the system of stability equations in the Dunn – Lin approximation was used with the boundary conditions of vanishing longitudinal, normal velocities and temperature of on the wall, disturbances, and their damping at infinity. The calculations were performed for the most unstable three-dimensional disturbances of the first mode, and for the two-dimensional (most unstable) disturbances of the second mode. The results are

(1)When the limits coefficient of disturbance amplification in an unstable region of the laminar boundary layer is set to be a definite value n; in the present case $n = 9$.

presented in Figs.1–2. The transition Reynolds number was determined from the ratio $R_t = (\mathrm{Re}_t)^{0.5} = (\mathrm{Re}_1 x_t)^{0.5}$, where Re_1 is the unit Reynolds number. As it follows from Fig.1, for $M > 7$ and $T_w = 1$, with increasing M the Reynolds number of transition, caused by both the first and the second (high-frequency) modes, increases. The surface cooling (Fig.2) stabilizes the first-mode disturbances and destabilizes the second-mode disturbances.

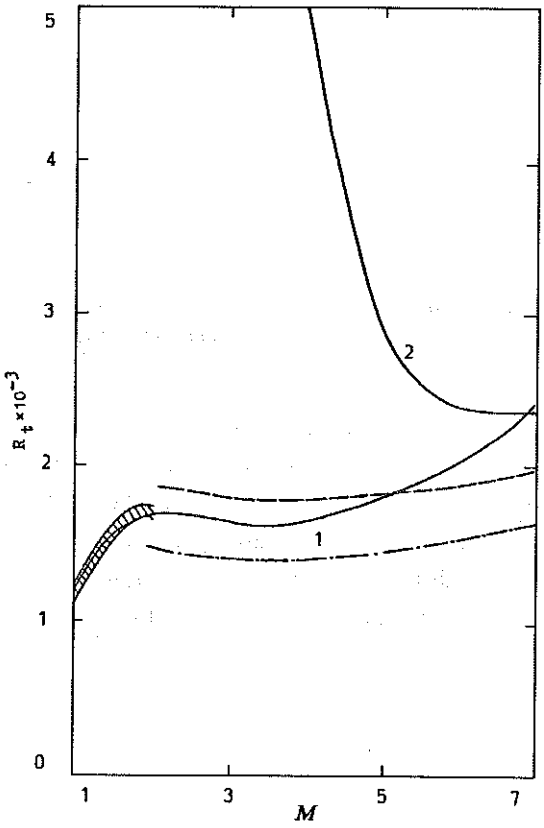

FIG. 1. Numerical Reynolds number of the transition on an insulated cone as a function of Mach number ($T_e = -50$ C): (1) for the first mode of disturbances; (2) for the second mode; ▨ – the flight data of FISHER and DOUGHERTY [12]; – – – – the ballistic data of BECKWITH and BERTRAM [13].

The influence of the stagnation temperature and velocity (pressure) gradient on the boundary-layer stability and the transition was also studied. This influence is shown in Figs. 3 and 4. The $F = 2\pi f/\mathrm{Re}_1 u_\infty$ is the dimensionless frequency parameter, with f being the disturbance frequency and u_∞ the velocity in the non-disturbed flow. The disturbance amplification

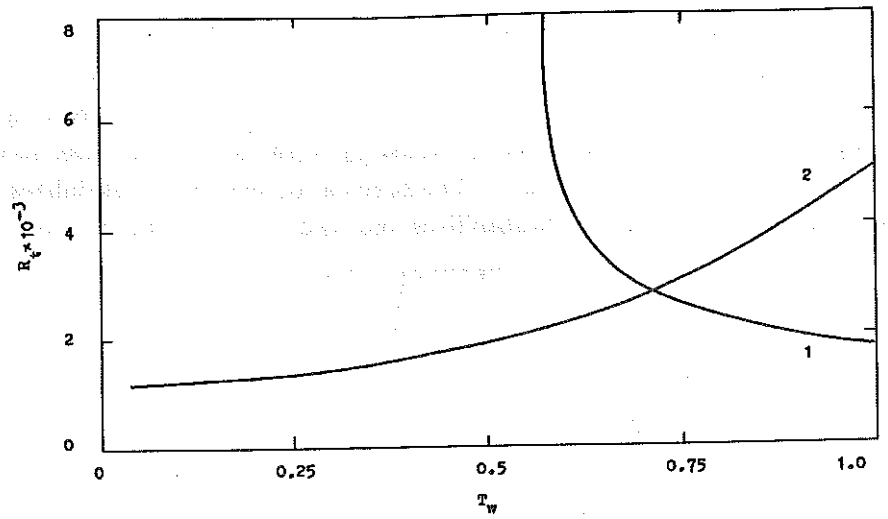

FIG. 2. Numerical transition Reynolds number in function of the temperature factor ($M = 4$, $T_0 = 937$ K): (1) for the first unstable mode; (2) for the second mode.

rates were determined from the relation: $\alpha_i = -0.5d(\ln A_f)/dR$, where A_f is the disturbance amplitude of the frequency f. The law of viscosity, as the function of temperature according to Sutherland, was used in the calculations. A local similarity in the boundary-layer flow was assumed. Figs. 3 and 4 illustrate the stabilizing effect of the stagnation temperature T_0 and the negative pressure gradient (positive β) on both the first- and the sec-

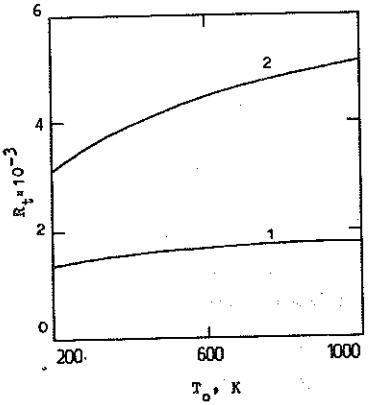

FIG. 3. Numerical transition Reynolds number as a function of the stagnation temperature ($M = 4$, $T_w = 1$): (1) for the first mode; (2) for the second mode of disturbances.

ond-mode disturbances. In particular, the effect on the second mode is more pronounced than on the first mode.

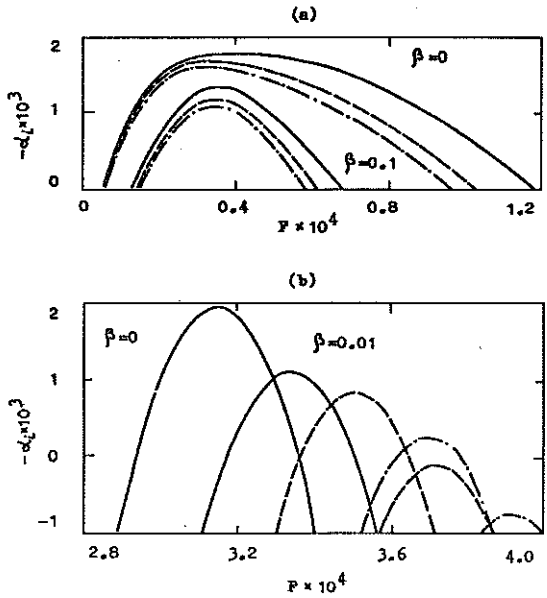

FIG. 4. Numerical disturbance amplification rates as functions of the frequency parameter at different negative pressure gradients (positive β) and different stagnation temperatures ($M = 4$, $T_w = 1$, $R = 780$): (a) first mode; (b) second mode; (——) – $T_0 = 300$ K; (– – –) – 600 K; (– · –) – 900 K.

The boundary-layer stability on a flat plate within the range of Mach numbers (at the boundary-layer bound) $M_e = 11 - 16$ was studied experimentally in the nitrogen tunnel T–327. The unit Reynolds number was $(\mathrm{Re}_1)_\infty = (u/\nu)_\infty = (0.7 - 1) \times 10^6\,\mathrm{m}^{-1}$, the stagnation temperature in the stilling chamber was $T_0 = 1100 - 1260$ K, and pressure in the stilling chamber was $(11.6 - 13.2) \times 10^6$ Pa (for details see LYSENKO [2]). The temperature factor varied due to the change of T_0. The nitrogen purity was 10 molecules of oxygen per million molecules of nitrogen. The length of a steel polished plate was 330 mm, the thickness 8 mm, the bevel angle of the leading edge 7°, and its bluntness $b = 0.1$ mm. The parameter of viscous interaction (between the boundary layer and the external inviscid flow) was larger than 1, i.e. a strong interaction took place. The measurements of the boundary-layer stability were carried out in the layer $u/u_e = 0.4$ with the help of the hot-wire anemometer of constant current and of the probes with tungsten wire of 6μm in diameter and 1.5 mm in length. The results of the

theory for the second (high-frequency) disturbances mode were confirmed qualitatively. It can be seen from Fig. 5 that the growth of Mach number exerts a stabilizing influence on the boundary-layer stability. The frequencies corresponding to the least stable disturbances decrease. The decrease in the

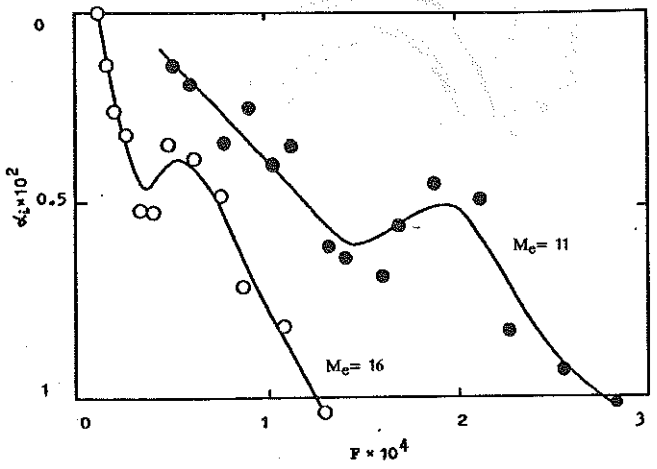

FIG. 5. Experimental disturbance amplification rates as functions of the frequency parameter for $T_w = 0.28 - 0.30$, $R = 481 - 558$, $M_e = 11$ and 16.

temperature factor (Fig. 6) has a destabilizing effect on the boundary-layer stability. This result corresponds to the result of LYSENKO and MASLOV [3]

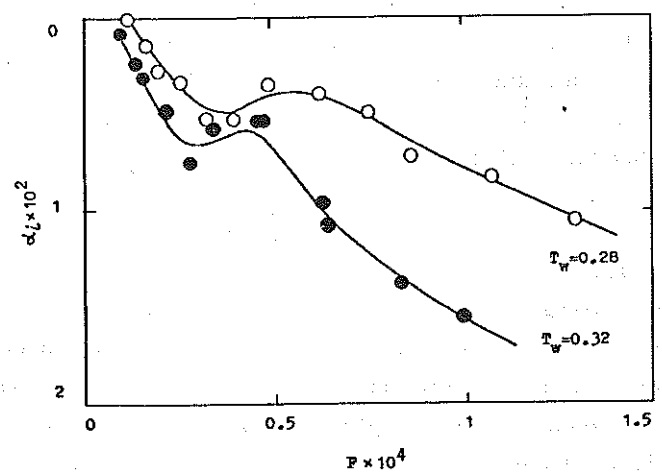

FIG. 6. Experimental amplification rates of disturbances as functions of the frequency parameter for $M_e = 16$, $R = 558 - 600$, $T_w = 0.28$ and 0.32.

on the effect of cooling upon the second-mode disturbances at $M = 4$. For $M_e = 11 - 16$ at $(\mathrm{Re}_x)^{0.5} \leq 600$, the flow on a smooth plate is stable, and the boundary layer is laminar.

3. The turbulization of the laminar hypersonic boundary layer by an obstacle

In the same nitrogen tunnel T–327 at $M_e = 16$, $(\mathrm{Re}_1)_\infty = (1.03 - 1.13) \times 10^6\,\mathrm{m}^{-1}$ and $T_0 = 1000 - 1060\,\mathrm{K}$, a study was carried out of the stable boundary-layer turbulization by means of an obstacle of a rectangular shape. The same plate served as a model but the obstacle was located at the distance of 60 mm apart from the leading edge. The obstacle height h varied and had the following values: 0, 1, 2, 3, 4, 5, 8, 10 and 15 mm. The thickness of the boundary layer δ on the plate without turbulator at the longitudinal coordinate $x = 60\,\mathrm{mm}$ was 11 mm, approximately. All the pneumometric measurements (including those used for fixation of the boundary-layer transition location) were carried out with the help of a strain gauge of the full pressure[2] with the inlet diameter of 2 mm. For $M_e = 16$ the dynamic pressure profiles were deformed in such a way that near the wall the dynamic pressure value was very small (contained within the limits of the gauge measurement error equal to $\pm 0.3\,\mathrm{kg/m^2}$). Then the measurements of the boundary-layer transition were carried out in the sections with the normal coordinates $y = 20$ and 10 mm within the range of $x = 100 - 318\,\mathrm{mm}$. In order to control the state of the boundary layer, the flow was visualized by means of a beam of fast electrons. Electrons being shot by electron gun, were falling on the nitrogen molecules and exciting them. Photons were then released and the luminescence (of violet colour) occurred. It was observed in the experiments (Figs. 7 and 8; where P_0' is the gauge-measured full pressure) that even a very stable boundary layer at large Mach numbers on a flat plate can be turbulized by an obstacle.

The following experiments were carried out in the wind tunnel T–325 on a flat insulated plate with an obstacle for $M_e = 4$, $T_0 = 290\,\mathrm{K}$ and $(\mathrm{Re}_1)_\infty = 11 \times 10^6\,\mathrm{m}^{-1}$. The hot-wire anemometer of constant current TPT–4 and the probes with tungsten wire of 6 μm in diameter and 1.5 mm in length were used. The profiles of mass flow disturbances $< m >$ and the profiles of average value u/ν were obtained. A steel polished flat plate of

[2] based on the gauge PG-10GC made by the KYOWA Electronic Instruments CO LTD

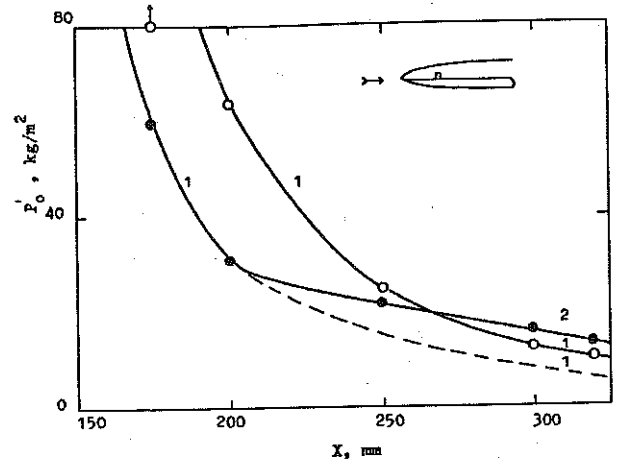

FIG. 7. Distribution of the gauge-measured full pressure along the streamwise coordinate for $M_e = 16$, the normal coordinate $y = 20$ mm and different values of the obstacle height: o – $h = 0$; • – $h = 15$ mm; (1) laminar boundary layer; (2) turbulent boundary layer.

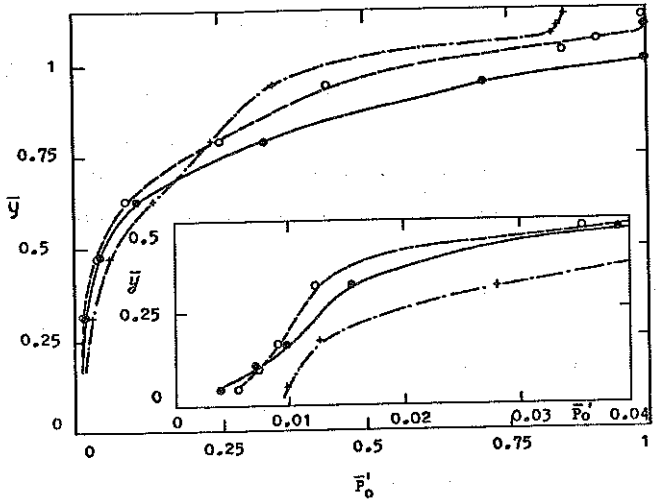

FIG. 8. Distribution of the gauge-measured full pressure across the boundary layer at different values of obstacle height, $M_e = 16$, $(\mathrm{Re}_1)_\infty = (1.03 - 1.13) \times 10^6$ m^{-1}, $x = 295$ mm; • – $h = 0$; o – 8 mm; + – 15 mm.

280 mm in length, 10 mm thick, with the bevel angle of the leading edge equal to 15° and its bluntness 0.1 mm, was used as a test model. A rectangular obstacle was located 41 mm apart from the leading edge. The obstacle height h had the following values: 0, 0.1, 0.2, 0.4, 0.8 and 1.2 mm (the thickness of

the boundary layer on the plate without turbulator at $x = 41$ mm was about 0.8 mm). The measurements were carried out in the section at $x = 123$ mm. It was observed that with an increasing h the thickness of the disturbed layer grew considerably and the profiles of u/ν were straightened. The maximum of the pulsations of the mass flow is situated at $y/\delta \approx 0.7$ for the laminar boundary layer. For the turbulent boundary layer (when $h = 0$) it is at $y/\delta \approx 0.5$ (Fig. 9), with $\eta = yR/x$ being the dimensionless normal coordinate. When h grows, the position of maximum (regarding the boundary of disturbed layer) changes only a bit. By the way, for all h the normal coordinate of this maximum $y_{<m>\max} > h$. The maximum intensity of the mass flow pulsations decreases with the transition from the laminar boundary layer to the turbulent one, then h/δ grows up to 1, remains on

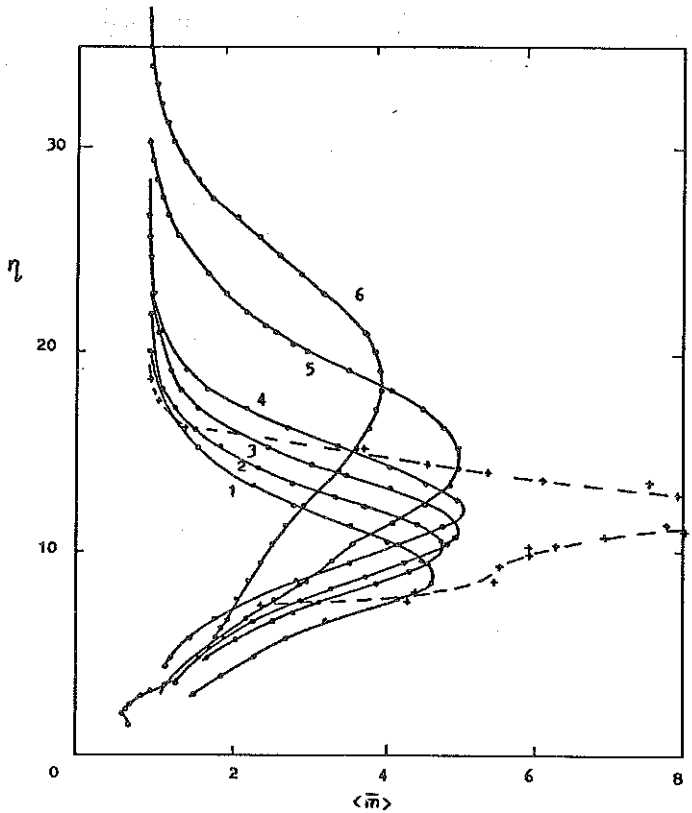

FIG. 9. Distribution of the mass-flow disturbances across the boundary layer at different dimensionless heights of the obstacle $M_e = 4$, $(\mathrm{Re}_1)_\infty = 11 \times 10^6\ \mathrm{m}^{-1}$, $x = 123$ mm: (+, – – –) – laminar boundary layer; (•, ——) – turbulent boundary layer; (1) $\bar{h} = 0$, (2) 0.12, (3) 0.25, (4) 0.5, (5) 1.0, (6) 1.5.

the same level (though an insignificant rising occurs), and decreases again with the further growth of h so that the profiles of the mass flow pulsations become steeper.

4. The influence of an entropy layer on the stability and the transition

The following experiments (the details in Lysenko [4]), were carried out at $M_\infty = 4$ in the wind tunnel T–325 on an insulated plate using the hot-wire anemometer of constant current TPT–4 and the probes with tungsten wire of 6 μm in diameter and 1.5 mm in length. The polished steel flat plate of 450 mm in length with the bevel angle of 20° was used as a test model. The leading-edge bluntness b had the following values: 0.1, 1, 1.5, 2, 3, 5 and 10 mm.

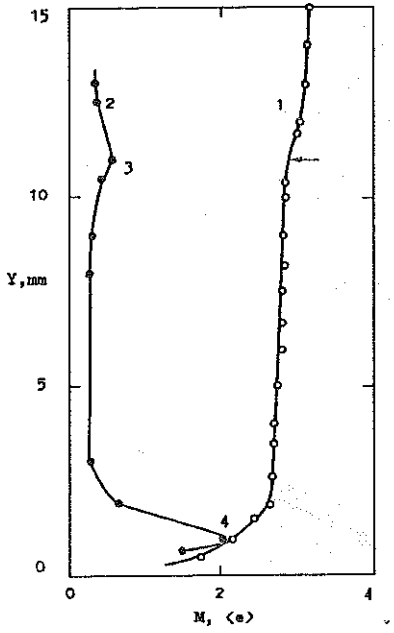

Fig. 10. Profiles of Mach number (1) and the hot-wire voltage fluctuations (2) in a shock layer for the plate leading-edge bluntness $b = 5$ mm, $M_\infty = 4$, $(\mathrm{Re}_1)_\infty = 25.3 \times 10^6\ \mathrm{m}^{-1}$, $x = 80$ mm; (3) entropy layer; (4) boundary layer.

The carried out experiments showed that the growth of an entropy layer with the increasing bluntness of the model destabilizes both the disturbances

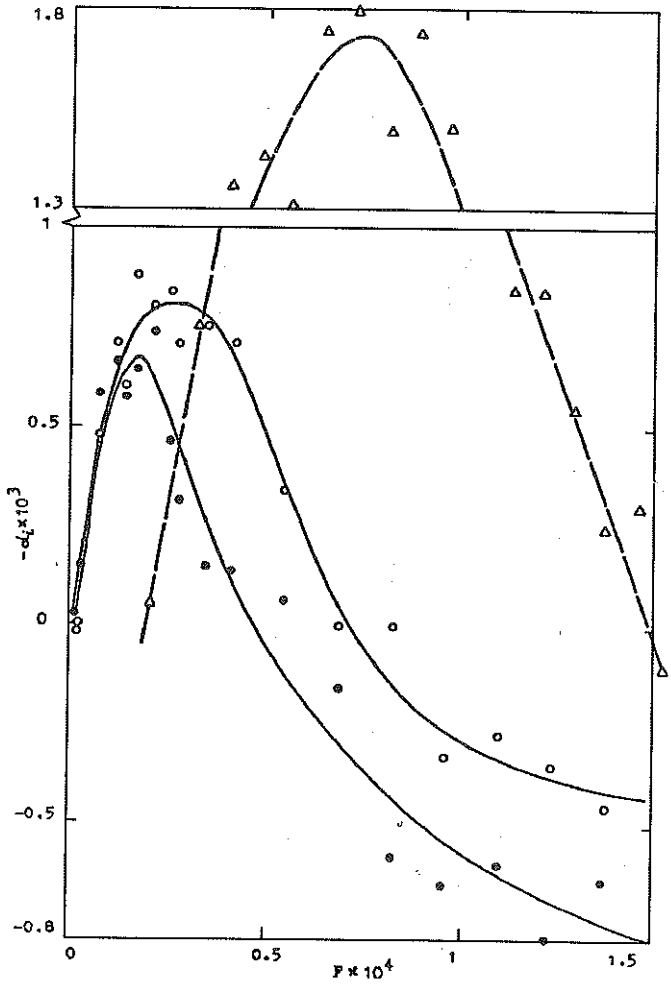

FIG. 11. Experimental boundary-layer disturbance amplification rates as functions of the frequency parameter for $M_\infty = 4$, $M_e = 2.7$, $(\mathrm{Re}_1)_e \approx 7.8 \times 10^6\ \mathrm{m}^{-1}$, $R_e = 765 - 780$, for different leading-edge bluntnesses: o – $b = 5$ mm; • – 3 mm; △ – 0.02 mm.

in the entropy layer (Figs. 10 and 12, $< e >$ - hot-wire voltage fluctuations) and (beginning at some bluntness) the first-mode disturbances in the boundary layer (Fig. 11). Thus at $M_\infty = 4$ the whole shock layer is destabilized. A clearly expressed reverse of the transition was observed in the dependence of the transition Reynolds number on the leading edge bluntness (Fig. 13). The comparison with the data for $M_\infty = 8$ allows to assume that with increasing Mach number the role of the entropy layer instability increases in a general instability of the whole shock layer.

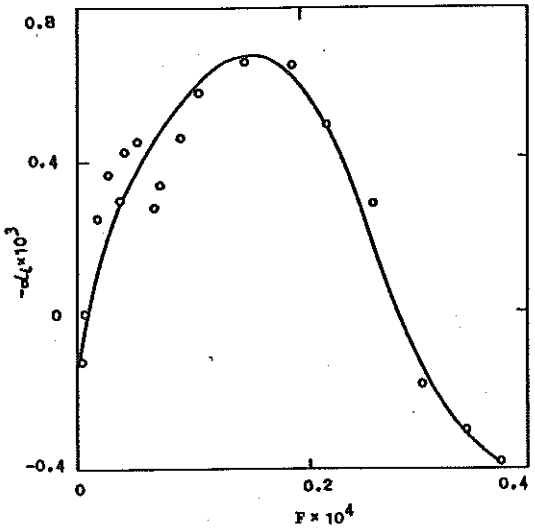

FIG. 12. Experimental amplification rates of the disturbances in an entropy layer as functions of the frequency parameter for $M_\infty = 4$, $(\mathrm{Re}_1)_\infty = 25.3 \times 10^6\ \mathrm{m}^{-1}$, $x = 80\ \mathrm{mm}$, $b = 5\ \mathrm{mm}$.

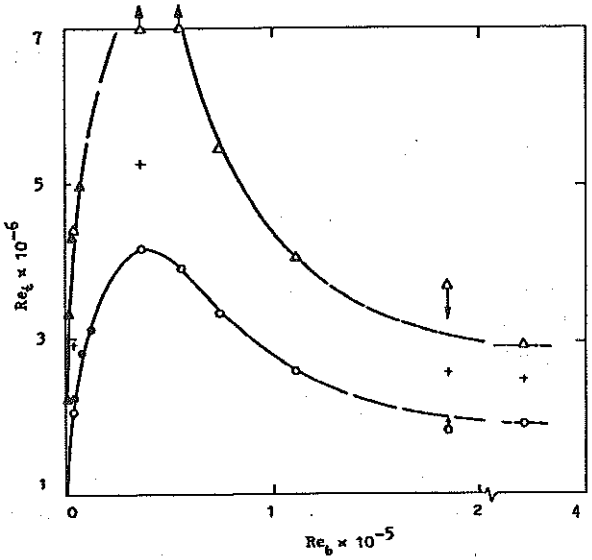

FIG. 13. Transition Reynolds number as function of the bluntness Reynolds number, $M_\infty = 4$, $(\mathrm{Re}_1)_\infty = 37 \times 10^6\ \mathrm{m}^{-1}$: o, • – full pressure gauge transition-onset data; ▲, △ – full pressure gauge transitione end data; + – hot-wire transition data.

5. The boundary-layer stability near a surface

The stability experiments usually are carried out by using hot-wire anemometer located inside a boundary layer (near a critical layer) both at subsonic and supersonic velocities. However, in the case of hypersonic velocities it may be preferable, because of the high stagnation temperature, the relatively high impact pressure and other reasons, to investigate the development of waves near a model surface. For these purposes, the film hot-wire probes and the pressure probes can be used. From the point of view of the parallel-flow stability theory the wave parameters obtained using the measurement results should coincide inside the boundary layer and on the surface. However, because of the non-parallelism of the flow in the boundary layer, the wave parameters are different at different distances from the surface. Moreover, they depend on the flow parameters which are measured.

The calculations and the experiments concerning the determination of the boundary-layer stability near the plate surface and near the critical layer (inside the boundary layer) were carried out (details in Gaponov and Lysenko [5]). The calculation results (by Gaponov) of the disturbance growth rates of the mass flow gradient, the temperature gradient and pressure on the plate surface were compared with the experimental data (of Lysenko) obtained using the hot-wire probes located on the model surface. The theoretical investigations of the disturbances development were based on the linearized Navier-Stokes equations with regard for a weak nonparallelism of the main flow. Experiments were carried out in the wind tunnel T-325. The stability of the boundary layer and the transition position were determined by means of the constant-current hot-wire anemometer TPT-3 and five hot-wire probes located on the plate surface (on ebonite substrates) at the distance of 10 mm one from another.

One of the series of experiments was performed at $M = 4.0$ and $R = 795$ ($\mathrm{Re}_1 = 6 \times 10^6\ \mathrm{m}^{-1}$). The measurement results (Fig. 14) were compared with the experimental data ($M = 4.0$, $R = 780$) obtained near the critical layer, as well as with the theoretical results ($M = 4.0$, $R = 780$, angle of disturbance propagation $\chi = 46°$) for the first unstable mode. It turned out that at $M = 2$ the experimental amplification rates of the disturbances near the model surface were less than those inside the boundary layer near the critical layer. At $M = 4$ they were approximately equivalent. It was observed that the temperature disturbances near the surface grow with M more intensively than the mass flow disturbances. In the case of the second

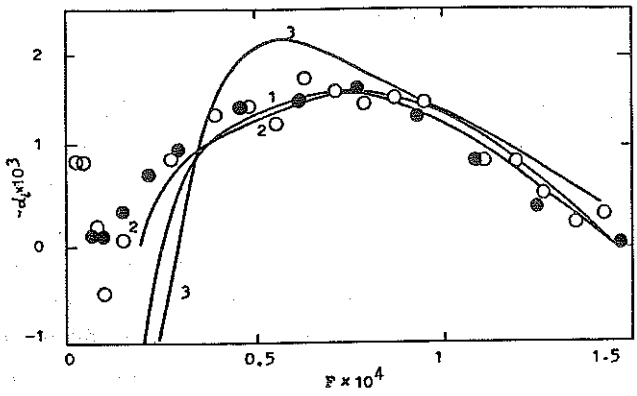

FIG. 14. Experimental and numerical disturbance amplification rates inside a boundary layer and near a surface vs. frequency parameter at $M = 4$, $R = 780 - 795$, o, • – hot-wire experiments; (——) – calculations; o – inside the boundary layer near a critical layer; • – near the plate surface; (1) maximum (in the boundary layer) mass-flow disturbances; (2) mass-flow disturbances near the surface; (3) temperature and stagnation-temperature disturbances near the plate surface.

unstable oscillation mode, the noticeable change of the pressure disturbances amplitude across the layer was the characteristic distinction from the data for the first mode (at $M = 2$ the first-mode pressure-oscillation growth rates were constant inside the boundary layer). For the second unstable mode of amplification rates of the disturbances of the mass flow, stagnation temperature, longitudinal velocity, temperature and pressure were almost equivalent near the plate surface.

6. THE INFLUENCE OF THE RATIO OF SPECIFIC HEATS ON THE STABILITY AND THE TRANSITION

The experiments and calculations regarding the influence of the ratio of specific heats on the stability and transition of the boundary layer were also carried out (for details see LYSENKO [6]). The experiments were performed in the hot-shot tunnel IT–302M at the Mach number $M_e \approx 4$, temperature factor $T_w = 0.18$ and stagnation temperature $T_0 \approx 1800$ K. The air, carbon dioxide, and argon were the test gases (the values of ratio of specific heats γ were 1.41, 1.2 and 1.67, respectively). A polished steel flat plate of 440 mm in length, 10 mm in thickness and with the bluntness of the leading edge equal to 0.1 mm was used as a test model. An optical method was employed

for fixation of the transition location. Using the Schlieren's shadow device with a cinema unit Pentazet–35 (the shooting frequency of 500 frames per second) the cinematographic records were obtained of the flow around a model by changing Re_1. The unit Reynolds number of the free stream varied within the range $(2 - 30) \times 10^6\,\mathrm{m}^{-1}$. Besides experiments, the calculations of boundary layer stability and its transition were performed by using the e^n method (see Sec. 2 of this paper) at different γ. The calculations were carried out for two-dimensional disturbances of the second unstable mode. For $M_e = 4$ and $T_w = 0.18$ precisely, the second mode determined the location of the boundary-layer transition, and the most unstable were two--dimensional disturbances.

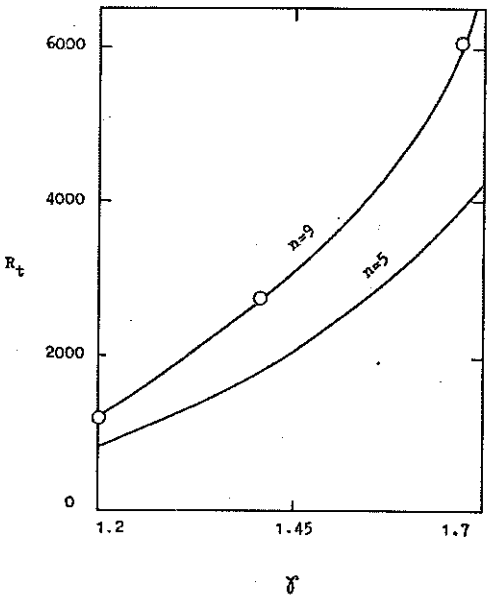

FIG. 15. Numerical Reynolds number of the flat-plate transition vs. the ratio of specific heats at two values of disturbance-amplification coefficient ($n = 5$ and 9) at $M = 4$ for second-mode disturbances: (——) – calculations at the Prandtl number $\sigma = 0.72$ and Sutherland constant $T_s = 110\,\mathrm{K}$; o – calculations for carbon dioxide ($\gamma = 1.2$, $\sigma = 0.64$, $T_s = 240\,\mathrm{K}$), air ($\gamma = 1.41$, $\sigma = 0.72$, $T_s = 110\,\mathrm{K}$) and argon ($\gamma = 1.67$, $\sigma = 0.75$, $T_s = 142\,\mathrm{K}$).

The calculations have shown that with decreasing γ the disturbances amplification rates increase considerably. The frequency of disturbances leading to the transition increases as well. Both experiments and calculations have shown (Figs. 15 and 16) that with the decreasing ratio of specific heats, the

Reynolds number of transition, depending on the disturbances of the second mode, decreases considerably.

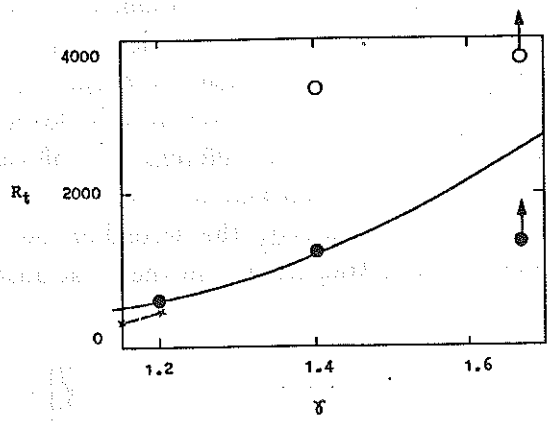

FIG. 16. Experimental and numerical transition Reynolds number as a function of the specific heats ratio $M_e = 4$ • – experiment, $\mathrm{Re}_1 = 4.5 \times 10^6\ \mathrm{m}^{-1}$; o – experiment, $\mathrm{Re}_1 = 40 \times 10^6\ \mathrm{m}^{-1}$; (——) – calculation at $n = 2.5$, × – the numerical data of PETROV [7] on absolute instability.

Figure 16 also demonstrates the calculation data of PETROV [7] of the absolute instability of the boundary-layer flow. When the extremely small initial disturbances begin to increase unlimitedly with time, it leads to the premature transition.

7. THE INFLUENCE OF DISSOCIATION, IONIZATION AND MAGNETIC FIELD ON THE TRANSITION

The following experiments were carried out aimed at the determination of the influence of dissociation and ionization of gases on the boundary-layer transition. The effect of dissociation was studied in the hotshot tunnel 302M, and the effect of ionization was examined in the shock tube UT-3 (for details consult LYSENKO [8]). When performing the studies in the hotshot tunnel 302M, the model and the instrumentation for transition fixation remained the same as in the previous series of experiments, but the free stream parameters varied. Air and nitrogen were the test gases. The free stream Mach number varied from 5 to 7 depending on the stagnation temperature (in particular, for temperatures higher than that of the oxygen dissociation, $M_\infty \approx 5$). The flow stagnation temperature T_0 varied within the range from

1100 up to 3600 K. The temperature factor $T_w = 0.32 - 0.10$. The unit Reynolds number $\mathrm{Re}_1 = (4.5 - 1.8) \times 10^6\,\mathrm{m}^{-1}$. At $T_0 \geq 2600$ K the oxygen, being a part of the air, started dissociating, and the dissociation of nitrogen did not occur within the range of the used temperatures. For these data of M and T_w, the flow instability was caused by the second mode disturbances. Experiments have shown (Fig. 17) that the gas dissociation at $M = 5$ and $T_w \approx 0.1$ leads to a decrease in the transition Reynolds number. It qualitatively corresponds to the computation results of PETROV [9, 10] for a case of external flow dissociation at moderate Mach number $M \lesssim 6$ (when the dissociation stabilizes first-mode oscillations and, on the contrary, destabilizes second-mode disturbances).

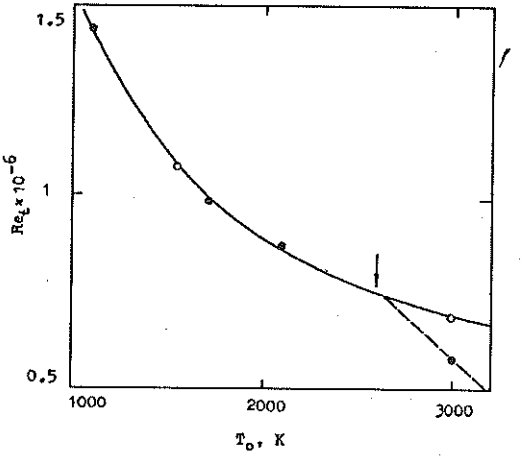

FIG. 17. Comparison of the transition Reynolds numbers for nitrogen and air at different stagnation temperatures: o – nitrogen; • – air; ↓ – temperature of oxygen dissociation.

In the shock tube the effect of gas ionization on the transition location on tube walls was examined. The test gases were argon and xenon. They are monoatomic gases with close ratios of specific heats (at the normal conditions equal to 1.67), but different ionization potentials (argon has a higher value of 15.76 ev as compared with 12.13 ev for xenon). The ionization of xenon began at the shock-wave Mach number $M_s \approx 8.6$, and that of argon at $M_s \approx 9.5$. The performed experiments have shown (Fig. 18, α – ionization rate) that the ionization of the flow at $M_s = 8 - 11$ leads to a weak increase in the transition Reynolds number on shock tube walls. It qualitatively corresponds to the computation results of PETROV [9] for the case of external flow dissociation at large Mach numbers $M \gtrsim 8$ (when the

dissociation already started exerting some stabilizing effect on the second mode disturbances).

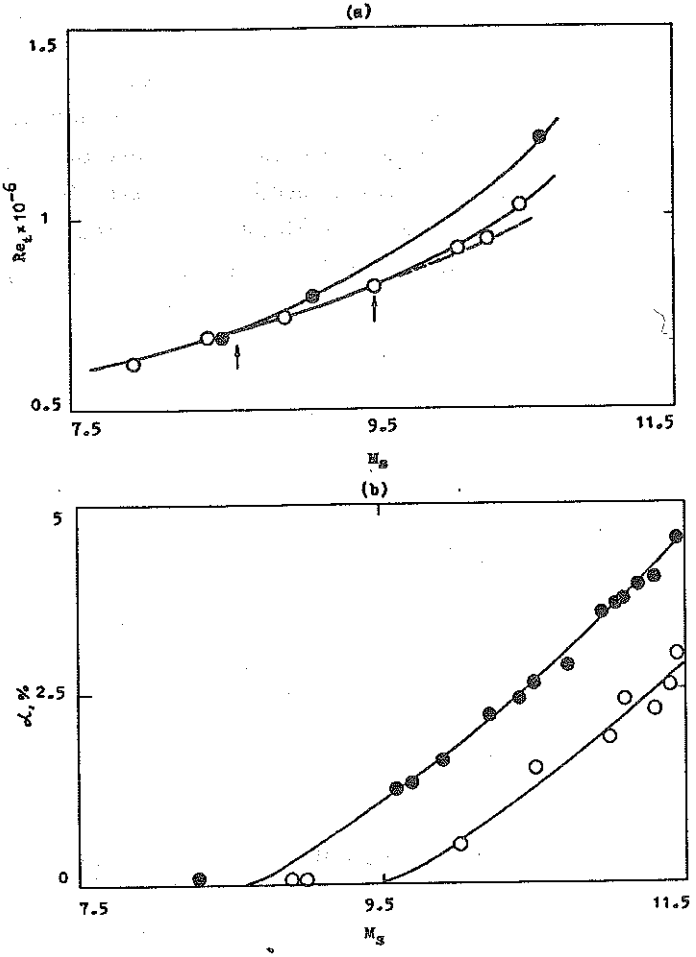

FIG. 18. Comparison of the transition Reynolds numbers (a) and ionization rates (b) for argon and xenon at different shock-wave Mach numbers: o – argon; • – xenon; ↑ – start of ionization (for xenon and argon).

The effect of the longitudinal magnetic field on the boundary-layer transition on a flat plate with an obstacle in the ionized gas was studied in the tunnel T–327 at $M_e = 16$ (details in KISELEV and LYSENKO [11]). A model and the instrumentation for the transition fixation were the same as in the Sec. 3. It can be seen (Fig. 19) that the longitudinal magnetic field stabilizes the boundary-layer disturbances, and the transition is delayed.

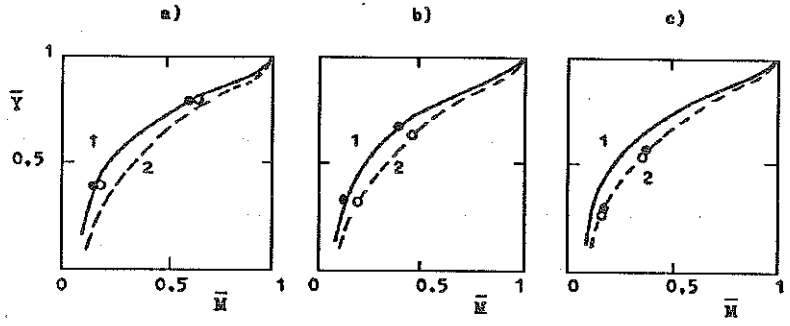

FIG. 19. Experimental profiles of the Mach number in the boundary layer on a flat plate with an obstacle, $M_e = 16$, (1) laminar boundary layer; (2) turbulent boundary layer; o – without magnetic field; • – with magnetic field, (a) $x = 200$ mm; (b) 250 mm; (c) 300 mm.

8. CONCLUSIONS

1. With the increasing Mach number and stagnation temperature the hypersonic boundary-layer stability increases, but the decreasing temperature factor and ratio of specific heats destabilizes the second-mode disturbances.

2. Such hypersonic effects as dissociation, ionization and the influence of a longitudinal magnetic field exert the stabilizing effect on the boundary-layer stability and the transition for $M > 8$. In other words, if in the calculations without consideration of these effects the boundary layer is laminar, it will be laminar in the calculations where those effects are included.

3. The very stable (at $M \sim 20$) hypersonic boundary layer can be turbulized by means of an obstacle on the flowed model surface.

REFERENCES

1. V.I.LYSENKO, *About a role of the first and the second modes of disturbances in the supersonic boundary-layer transition* [in Russian], Zh. Prikl. Mekh. Tekh. Fiz., **58**, 6, 1985.

2. V.I.LYSENKO, *High-speed boundary-layer stability* [in Russian], Zh. Prikl. Mekh. Tekh. Fiz., **76**, 6, 1988.

3. V.I.LYSENKO and A.A.MASLOV, *The effect of cooling on supersonic boundary-layer stability*, J. Fluid Mech., **147**, 39, 1984.

4. V.I.LYSENKO, *Influence of an entropy layer on the supersonic shock layer stability and laminar-to-turbulent boundary-layer transition* [in Russian], Zh. Prikl. Mekh. Tekh. Fiz., **74**, 6, 1990.

5. S.A.GAPONOV and V.I.LYSENKO, *Development of disturbances near a surface flowed by supersonic flow* [in Russian], Zh. Prikl. Mekh. Tekh. Fiz., **70**, 6, 1988.

6. V.I.LYSENKO, *The investigation of influence of ratio of specific heats on the supersonic boundary-layer stability and transition* [in Russian], Izv. Akad. Nauk SSSR, Mekh. Zhid. Gaza, **179**, 2, 1989.

7. G.V.PETROV, *The effect of a shock wave limited by a hypersonic shock layer on boundary-layer stability* [in Russian], [In:] Instability of Sub- and Supersonic Flows, 25–34, ITAM SO AN SSSR, Novosibirsk 1982.

8. V.I.LYSENKO, *The investigation of influence of gases dissociation and ionization on the supersonic boundary-layer transition* [in Russian], Izv. SO AN SSSR, Ser. Tekh. Nauk, **45**, 2, 1989.

9. G.V.PETROV, *The effect of dissociation on boundary-layer stability* [in Russian], [In:] Development of Disturbances in a Boundary Layer, 104–117, ITAM SO AN SSSR, Novosibirsk 1979.

10. G.V.PETROV, *Stability characteristics of a boundary layer of gas recombined on a cooled wall* [in Russian], Izv. SO AN SSSR, Ser. Tekh. Nauk, **8**, 2, 36, 1983.

11. V.YA.KISELEV and V.I.LYSENKO, *The effect of a longitudinal magnetic field on the high-speed boundary-layer transition* [in Russian], Izv. Akad. Nauk SSSR, Mekh. Zhid. Gaza, **183**, 4, 1991.

12. D.F.FISHER and N.S.DOUGHERTY Jr., *In-flight transition measurement on a 10° cone at Mach numbers from 0.5 to 2.0*, NASA-TP-1971, 1982.

13. I.E.BECKWITH and M.H.BERTRAM, *A survey of NASA Langley studies on high-speed transition and the quiet tunnel*, NASA-TM-X-2566, 1972.

SIBERIAN BRANCH OF THE RUSSIAN ACADEMY OF SCIENCES
INSTITUTE OF THEORETICAL AND APPLIED MECHANICS,
NOVOSIBIRSK, RUSSIA.

Received June 3, 1992.